Electronic Supplementary Material (ESI) for Journal of Materials Chemistry C.

Crystallinity and piezoelectric properties of spray-coated films of P(VDF_{70}-$TrFE_{30}$): effect of film thickness and spin-crossover nanofillers

José Elías Angulo-Cervera,[a,b] *Mario Piedrahita-Bello,*[a,b] *Baptiste Martin,*[a,c] *Eric Dantras,*[c] *Liviu Nicu,*[b] *Thierry Leichle,*[b,d] *Kevin Dalla Francesca,*[e] *Antonio Da Costa,*[e] *Anthony Ferri,*[e] *Rachel Desfeux,*[e] *Lionel Salmon,*[a] *Gábor Molnár*[a,*] *and Azzedine Bousseksou*[a,*]

[a] LCC, CNRS & University of Toulouse, 205 route de Narbonne, Toulouse 31077, France.

[b] LAAS, CNRS & University of Toulouse, 7 avenue du Colonel Roche,Toulouse 31400, France

[c] CIRIMAT, CNRS & University of Toulouse (UPS, INPT), 118 Route de Narbonne, 31062 Toulouse, France

[d] Georgia Tech-CNRS International Research Laboratory, School of Electrical and Computer Engineering, Atlantic Drive, Atlanta, GA, 30332,USA

[e] Univ. Artois, CNRS, Centrale Lille, Univ. Lille, UMR 8181 – UCCS – Unité de Catalyse et Chimie du Solide, F-62300 Lens, France

* Corresponding authors at: Laboratoire de Chimie de Coordination (LCC), 205 route de Narbonne, 31077 Toulouse cedex 4, France. E-mail adresses : gabor.molnar@lcc-toulouse.fr (G. Molnar) and azzedine.bousseksou@lcc-toulouse.fr (A. Bousseksou)

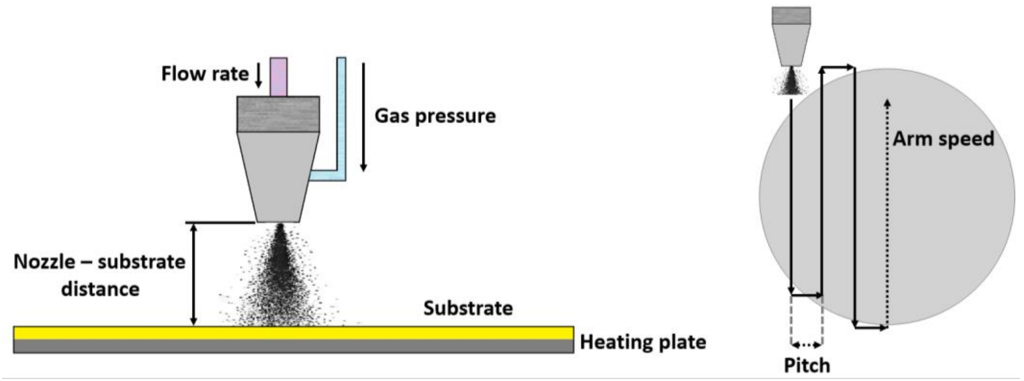

Fig. S1. Definition of spray coating parameters. While spray-coating is seemingly straightforward, optimization of parameters if often delicate. High flow rates can lead to a solvent "flooding" over the substrate resulting in non-homogeneous films, whereas low rates gave rise to early solvent evaporation that generates spider-web-like fibers. As in most solution deposition methods, the viscosity and concentration of the solution (which are interlinked) is a key issue. For composites, a stable dispersion of particles must be ensured due to the relatively long transit times. Generally, the viscosity must be low to guarantee fine micro-droplet formation. The main operation parameters that control the spray nozzle include the flow rate, which controls the amount of solution sprayed per time, the gas pressure, which controls the radius of the spray cone and the nozzle distance, which helps to regulate the airflow inside topographic features. The meander parameters (pitch and arm speed) define the movement of the nozzle relative to the substrate. The speed of the spray arm, together with the flow rate, define primarily the amount of resist deposited locally during one scan. Finally, by adjusting the temperature of the chuck, it is possible to control the rate of solvent evaporation as well as to stabilize the film right after the droplet deposition.

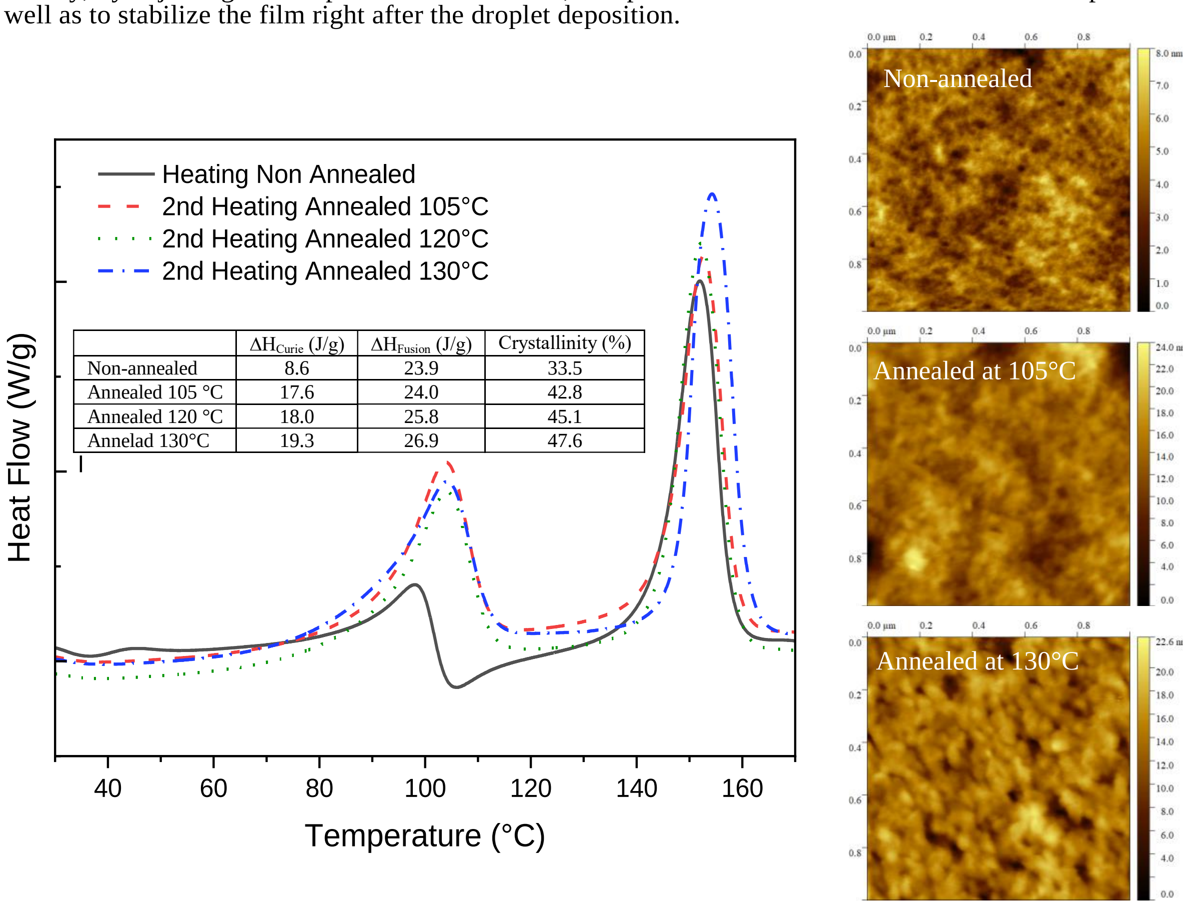

	ΔH_{Curie} (J/g)	ΔH_{Fusion} (J/g)	Crystallinity (%)
Non-annealed	8.6	23.9	33.5
Annealed 105 °C	17.6	24.0	42.8
Annealed 120 °C	18.0	25.8	45.1
Annelad 130°C	19.3	26.9	47.6

Fig. S2. DSC and AFM investigation of the effect of annealing temperature on the crystallinity of a 4 µm thick spray-coated $P(VDF_{70}\text{-}TrFE_{30})$ film. Left panel: DSC traces. The film was peeled away from the substrate and loaded into four DSC crucibles. The first crucible ('non-annealed') was directly heated to 170 °C at a rate of 10 °C/min. The three other crucibles were first annealed for 2 hours at 105 °C, 120 °C and 130 °C. respectively. then cooled back to 20 °C and finally heated to 170 °C at a rate of 10 °C/min. The table in insert shows the integrated peak areas and calculated crystallinity values. Right panel: AFM topography images acquired before annealing and after annealing at 105 °C and 130 °C. respectively.

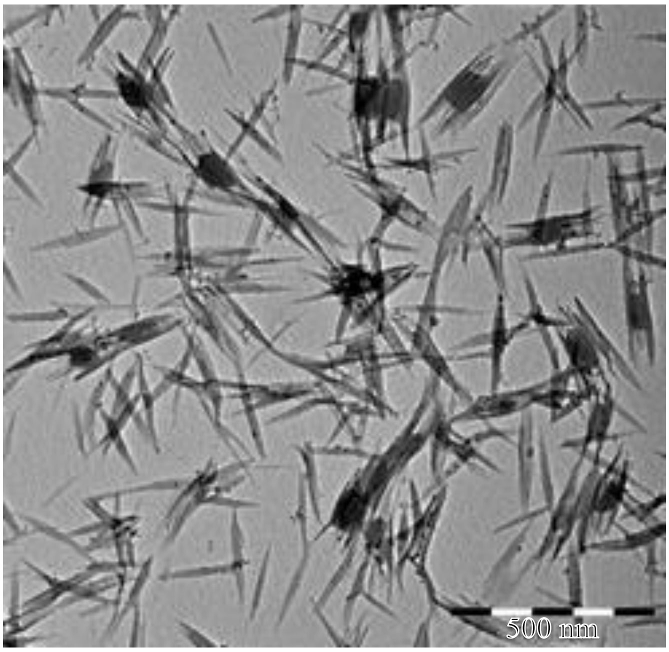

Fig. S3. Representative TEM image of the SCO particle filler

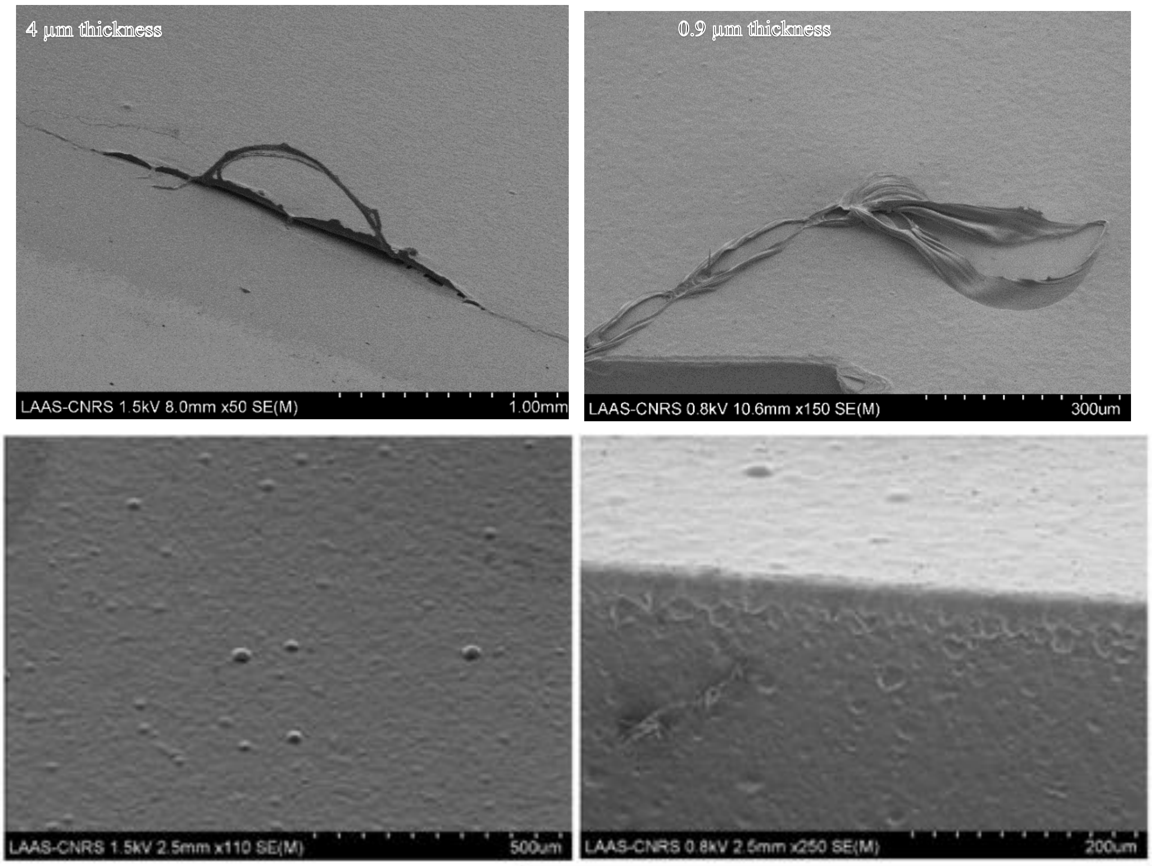

Fig. S4. Representative SEM images of the P(VDF-TrFE) films

0.2 µm thickness

0.8 µm thickness

4.0 µm thickness

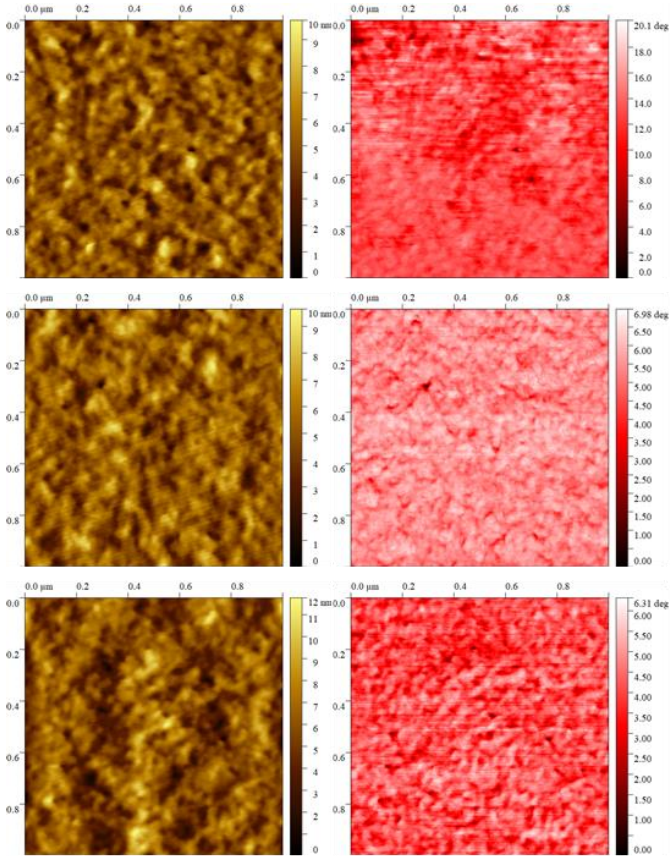

Fig. S5. Representative AFM images (topography and phase) of the annealed P(VDF-TrFE) films

0.3 µm thickness

0.9 µm thickness

3.8 µm thickness

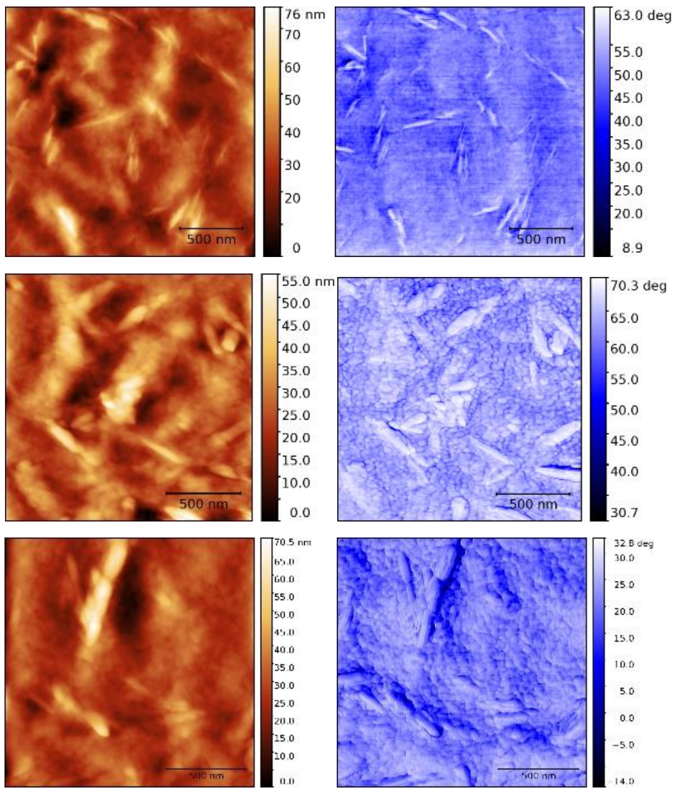

Fig. S6. Representative AFM images (topography and phase) of the annealed composite films (scale bars: 500 nm).

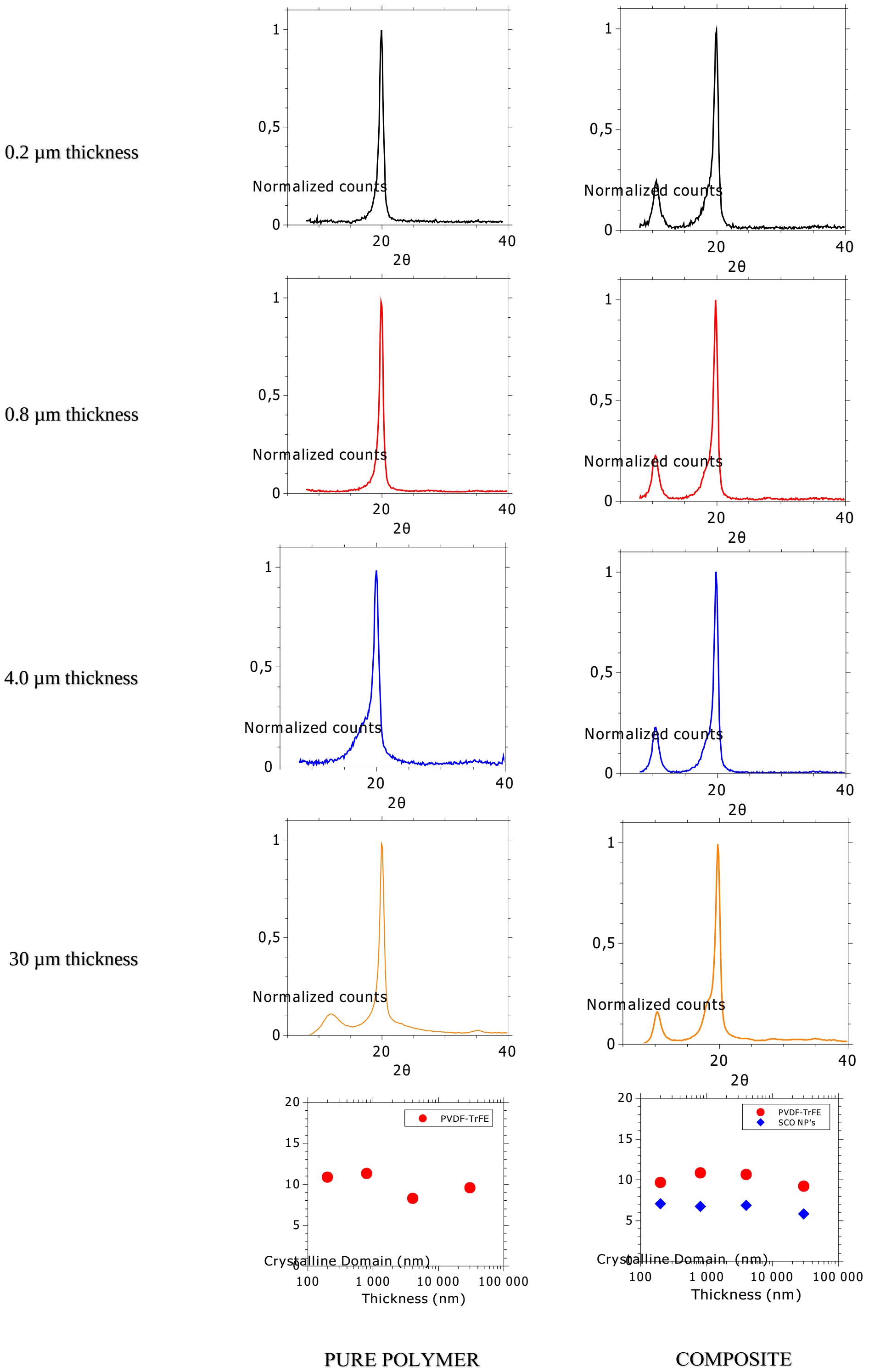

Fig. S7. XRD analysis on different films. Note that the 30 µm films were analyzed in a Bragg-Brentano geometry, whereas the other films were investigated in GI-XRD configuration.

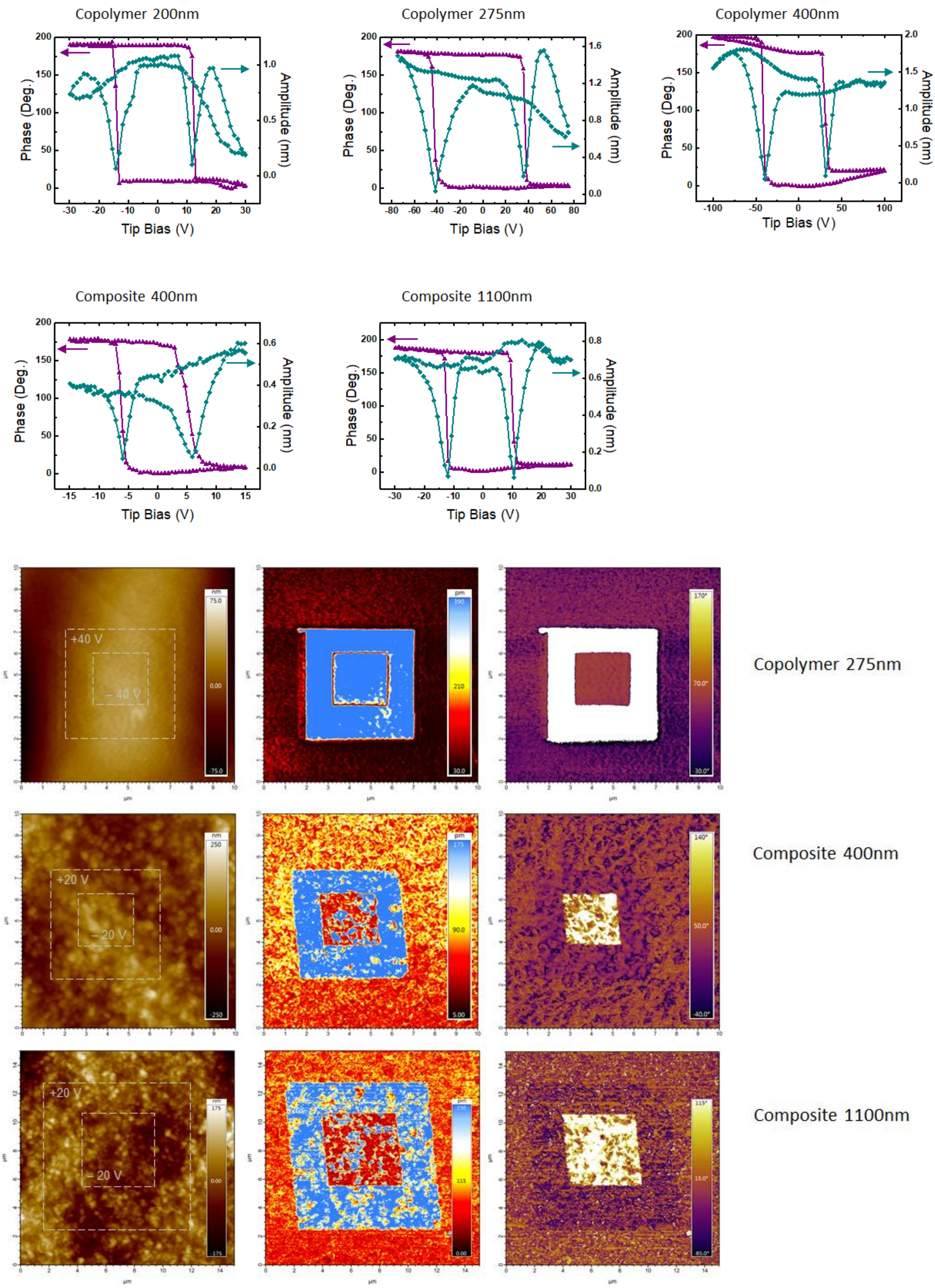

Fig. S8. PFM analysis of the different films